

Journal of Materials Chemistry A

Accepted Manuscript



This is an *Accepted Manuscript*, which has been through the Royal Society of Chemistry peer review process and has been accepted for publication.

Accepted Manuscripts are published online shortly after acceptance, before technical editing, formatting and proof reading. Using this free service, authors can make their results available to the community, in citable form, before we publish the edited article. We will replace this *Accepted Manuscript* with the edited and formatted *Advance Article* as soon as it is available.

You can find more information about *Accepted Manuscripts* in the [Information for Authors](#).

Please note that technical editing may introduce minor changes to the text and/or graphics, which may alter content. The journal's standard [Terms & Conditions](#) and the [Ethical guidelines](#) still apply. In no event shall the Royal Society of Chemistry be held responsible for any errors or omissions in this *Accepted Manuscript* or any consequences arising from the use of any information it contains.

Cite this: DOI: 10.1039/c0xx00000x

ARTICLE TYPE

www.rsc.org/xxxxxx

Ionic semi-interpenetrating networks as new approach for highly conductive and stretchable polymer materials

Alexander S. Shaplov,^{a*} Denis O. Ponkratov,^a Petr S. Vlasov,^b Elena I. Lozinskaya,^a Lyudmila V. Gumileva,^a Christine Surcin,^c Mathieu Morcrette,^c Michel Armand,^c Pierre-Henri Aubert,^d Frédéric Vidal^d and Yakov S. Vygodskii^a

Received (in XXX, XXX) Xth XXXXXXXXX 20XX, Accepted Xth XXXXXXXXX 20XX

DOI: 10.1039/b000000x

The synthesis and characterization of ionically conductive polymer films with high stretchability and good elasticity based on ionic semi-interpenetrating polymer networks (semi-IPNs) are discussed. Such innovative semi-IPN materials were prepared by radical copolymerization of ionic monomer, namely (N-[2-(2-(methacryloyloxy)ethoxy)ethoxy]ethyl)-N-methylpyrrolidinium bis(fluorosulfonyl)imide) with poly(ethylene glycol)(di)methacrylates in the presence of the dissolved nitrile butadiene rubber, ionic liquid and lithium salt, using a simple one-step process. The suggested approach allows for simultaneous imparting of high ionic conductivity ($1.3 \times 10^{-4} \text{ S cm}^{-1}$ at 25°C) and excellent mechanical properties (tensile strength up to 80 kPa, elongation up 60%) to a single polymer material. Ionic semi-IPNs, possessing unusual “Emmentaler cheese” like structure, exhibit wide electrochemical stability window (4.9 V) and acceptable time-stable interfacial properties in contact with metallic lithium. Preliminary battery tests have shown that Li/LiFePO₄ solid-state cells are capable to deliver a 77 mA h g⁻¹ average specific capacity at 40°C during 75 charge/discharge cycles.

Introduction

Elastic and conductive polymer materials are perspective for the creation of stretchable electronics,¹⁻⁹ particularly, for rechargeable batteries, solar cells, sensors, actuators, anti-radar devices, antistatic coatings, as a shielding material for protection from electric field and microwave radiation, self-regulating heaters, over-current protection coatings, etc.^{1,2,10,10-12}

One of the most common methods to impart conductivity, independently on its nature (ionic or electronic), to polymeric materials is the utilization of highly conductive fillers. Carbon black, carbon nanotubes, conjugated polymers, various metal salts and ionic liquids (ILs) can be named among the commonly used fillers.^{10,13-15} The conductivity of the polymer/filler composite can increase several orders of magnitude, when the filler content exceeds a critical value (percolation threshold). Thus, when particle concentration is higher than the percolation threshold, the filler particles are close enough to each other and the transfer of ions or electrons from one particle to the neighboring one becomes possible.^{16,17} However, high filler content makes processing of the material difficult and worsens mechanical properties, especially the tensile strength and elongation.¹⁰ When liquid filler, such as ILs, is used the problem of electrolyte retention from the polymer film upon repeated mechanical bending (stress) becomes obvious. Moreover, the increase in IL's content leads not only to the rise of the composite's conductivity, but also to the partial solubilization of

the polymer formation of the swollen polymer gels.¹⁸⁻²¹

Another approach for the preparation of conductive polymer films with high stretchability and elasticity consists in the formation of the conductive polymer layer on the surface of mechanically strong polymers (polypropylene, polycarbonate, epoxies, etc.).²² The thin conductive layer can either be deposited by spin-coating of the semiconducting polymer, such as polythiophenes, or is formed by polymerization of the respective monomer on the surface of elastomer film.^{4,22-25} The drawbacks of this method are the complexity of polymer layers compatibility, the appearance of wrinkles on conductive coating under bending deformations and lack of resistance to abrasion.

At present, poly(ionic liquid)s or polymeric ionic liquids (PILs) are considered as one of the perspective approaches to avoid problems with filling and at the same time to impart sufficient conductivity to polymer. PILs refer to a novel subclass of polyelectrolytes having ionic liquid species in every monomer repeating unit.²⁶⁻³³ Such polymers combine all beneficial properties of ILs with those of classical polyelectrolytes. Depending on the nature of ionic moieties, the type of spacer between the main chain and attached ions as well as the kind of a polymer backbone one can greatly vary PILs properties: ionic conductivity (from 10^{-11} to $10^{-5} \text{ S cm}^{-1}$ at 25°C³⁰), heat resistance (T_g from -8 to 70°C^{27,30,34-39}), thermal stability (from 165 to 350°C³¹), etc. However, despite all the advantages of PILs, there is an inverse relationship between the film's conductivity and its toughness, resulting in the loss of mechanical properties (sticky

rubberlike masses) when approaching a certain conductivity level ($>10^{-6}$ S cm $^{-1}$ at 25°C).^{30,38}

The present work deals with the continuation^{21,23,25,38} of the development of the synthetic methods for the formation of stretchable highly conductive polymer films based on ionic liquid like monomers (ILMs).^{40,41} The offered homogeneous polymer materials were obtained in one step by copolymerization of N-[2-(2-(2-(methacryloyloxy)ethoxy)ethoxy)ethyl]-N-methylpyrrolidinium bis(fluorosulfonyl)imide with poly(ethylene glycol) dimethacrylate (PEGDM) and poly(ethylene glycol) methyl ether methacrylate (PEGM) in the presence of the dissolved nitrile butadiene rubber (NBR), ionic liquid and lithium salt. Such polymer films represent semi-interpenetrating ionic networks (semi-IPNs), where the networked copolymer acts as a polyelectrolyte and a host matrix, while the reinforcement is provided by NBR. The choice of PEGDM and PEGM as comonomers for the creation of ionic network was driven by our previous results on the synthesis of conductive materials^{21,24,25,42} along with the example of highly conductive polyethylene glycol-polyurethane semiIPNs.⁴³ In contrast to our previous reports on the synthesis of conductive ionic interpenetrating networks (IPNs),^{21,24,25,42} and to the report on the development of semi-IPNs based on thermally-cured polyimide/polyvinyl pyrrolidone as nanoencapsulated-cathode materials,⁴⁴ the suggested approach is more simple, requires less amount of IL filler and opens new possibilities for the creation of highly conductive (up to 10^{-4} S cm $^{-1}$ at 25°C), solid and elastic (elongation at break up to 60%) films suitable for stretchable electronics.

Experimental Section

Materials

Poly(ethylene glycol) dimethacrylate (PEGDM, $M_n = 750$ g mol $^{-1}$, Aldrich), poly(ethylene glycol) methyl ether methacrylate (PEGM, $M_n = 475$ g mol $^{-1}$, Aldrich), nitrile butadiene rubber (NBR, $M_n = 80$ 100 g mol $^{-1}$, $M_w = 230$ 000 g mol $^{-1}$, 44 wt. % acrylonitrile units, Perbunan 4456F Lanxess), dicyclohexylperoxydicarbonate (DCPD, Groupe Arnaud), 2-[2-(chloroethoxy)-ethoxy]ethanol (98+%, TCI Europe), potassium bis(fluorosulfonyl)imide (98%, Solvionic), N-propyl-N-methylpyrrolidinium bis(fluorosulfonyl)imide ([N-Me-N-PrPyr](FSO $_2$) $_2$ N, 99.9%, Solvionic), lithium bis(trifluoromethylsulfonyl)imide (LiTFSI, 99+%, Solvionic, France), lithium chloride (99+%, Acros), phosphorus pentoxide (98%, Alfa Aesar), N,N-dimethylformamide (DMF, anhydrous 99.8%, Acros), 1,1,2-trichloroethane (97%, Aldrich), Li foil (1 mm thickness, Aldrich) and LiFePO $_4$ (Advanced Lithium Electrochemistry Co. Ltd., Taiwan) were used as received. Metacryloyl chloride (Fluka, 98%) was distilled over linseed oil, while N-methylpyrrolidine (99%, Acros) was distilled under inert gas over CaH $_2$. Dichloromethane, acetonitrile and diethyl ether were distilled over P $_2$ O $_5$. 2,2'-Azobisisobutyronitrile (AIBN, 98%, Acros) was recrystallized from methanol. Carbon black (Ketjen black EC-600JD, Azko Nobel) was dried at 80 °C/1 mm Hg for 12 h prior to use.

Characterization

Molar mass determination of PIL was studied by gel permeation chromatography (GPC) in 0.5M NaNO $_3$ aq. solution. For this purpose the synthesized PIL was exchanged to polymer with chloride anions: the solution of anhydrous lithium chloride (0.18 g, 4.28 mmol) in 15 mL of anhydrous DMF was added dropwise under inert atmosphere to the solution of PIL (1.00 g, 2.14 mmol) in 20 mL of DMF. The precipitation of the PIL in its chloride form was observed, whereupon it was collected by filtration, washed with DMF and purified by dialysis (Spectra/Por dialysis membrane, molecular weight cut off from 6000 to 8000) firstly in 0.5M aq. NaCl and then in deionized water. The final polymer solution was freeze-dried and chloride PIL was studied by GPC: $M_w = 4.2 \times 10^5$, $M_w/M_n = 4.7$. GPC experiments were performed at 30°C on a LC-20AD gel permeation chromatograph (Shimadzu Corporation, Japan) equipped with a Tosoh TSK-GEL G6000 PW $_{XL}$ -CP column and a refractive index detector. 0.5M NaNO $_3$ aq. solution was used as an eluent with a flow rate of 0.5 mL min $^{-1}$. The calibration was made with pullulan standards (Shodex P-82).

Intrinsic viscosity $[\eta]$ of PIL was measured in an Ubbelohde type capillary viscometer at 25.0°C using 0.5M K(FSO $_2$) $_2$ N solution in DMF.

NMR spectra were determined in CDCl $_3$ with Bruker AMX-300 spectrometer at 25 °C. Chemical shifts (δ) are reported in ppm downfield from tetramethylsilane, while CHCl $_2$ F was used as an internal standard for 19 F NMR. A Nicolet Magna-750 Fourier IR-spectrometer was used to record IR spectra at a resolution of 2 cm $^{-1}$ and with the scan number equal to 128 (KBr pellets).

DSC study of ILM was performed on a Q100 isothermal differential calorimeter (TA Instruments, USA) in the range from -90 to +100°C at a heating rate of 2.0 °C min $^{-1}$. T_g of PIL was determined by thermomechanical analysis (TMA) using Q400 analyzer (TA Instruments, USA) at a heating rate of 5 °C min $^{-1}$ and a constant load of 0.08 MPa. Dynamic Mechanical Thermal Analysis (DMTA) measurements were carried out on semi-IPN films (typically length \times width \times thickness = 15 \times 8 \times 0.2 (mm)) with a Q800 model (TA Instruments, USA) operating in tension mode (strain between 0.05 and 0.07 %, pretension: 10^{-2} N). Experiments were performed at 1 Hz frequency with a heating rate of 3°C min $^{-1}$ from -100 to 90°C. The set up provided the storage and loss modules (E' and E''). The damping parameter or loss factor ($\tan\delta$) was defined as the ratio $\tan\delta = E''/E'$. Thermal stability of PIL and semi-IPNs was studied by thermogravimetric analysis (TGA) in air on a Q50 model (TA Instruments, USA) applying a heating rate of 5 °C min $^{-1}$.

Mechanical properties of ionic semi-IPNs: δ_t - tensile strength (kPa), E_t - tensile modulus (kPa) and ϵ - elongation (%) were estimated at r.t. using dynamometer "Polyani" (Polyani, Hungary).

Transmission Electron Microscopy (TEM) was performed on Hitachi H-800 microscope. The samples were previously cut by cryo-ultramicrotomy and then exposed to osmium tetroxide

steam for 20 min.

Ionic conductivity and interfacial stability with lithium anode were determined by impedance spectroscopy with a VSP potentiostat (Bio-Logic Science Instruments, France). PIL and semi-IPNs were sandwiched between stainless steel electrodes (conductivity tests) or between lithium electrodes (interfacial stability tests) and sealed under inert atmosphere (Ar) in a metal CR2016 coin-type cell. For both experiments the cells were put in a thermostat (Buchi, Switzerland). The conductivity measurements were performed at 25°C, while the interfacial stability was studied at 25 and 40°C. For conductivity vs temperature dependence the experiments were carried out in a temperature range from 25 to 130°C with steps of 8-9°C. The runs were performed varying the frequency from 10⁻² to 10⁶ Hz with a rate of 6 points per decades and an oscillation potential of 10 mV.

The electrochemical stability window (ECW) of polyelectrolytes was evaluated by linear sweep voltammetry under argon atmosphere in a glove box (Jacomex, France) at r.t. using EG&G 273A (Princeton Applied Research, USA) potentiostat/galvanostat. Two equal films were assembled to make the following layered sequence: Li^o/polymer film/Pt or Ni/polymer film/ stainless steel grid, that was further placed under the pressure contacts. The ECW tests against Li/Li⁺ were performed by scanning at 1 mV s⁻¹ from the open circuit potential (OCP) toward positive (using Pt working electrode) or negative (using Ni working electrode) potentials. The contact area of electrodes was 0.2 cm².

The cycling tests on Li/semi-IPN2c/LiFePO₄ polymer batteries were performed at 40 °C using VMP-3 battery tester (Bio-Logic Science Instruments, France). The discharge current rates ranged from C/50 (0.036) to C/3.8 (0.48 mA cm⁻²) while the charge rate was fixed to C/50. The voltage cut-offs were fixed at 2.0V (discharge step) and 4.5V (charge step), respectively.

Ionic liquid monomer (ILM)

N-[2-(2-(2-methacryloyloxy)ethoxy)ethoxy)-ethyl]-N-methylpyrrolidinium bis(fluorosulfonyl)imide was prepared in a similar manner as its imidazolium analogues published previously.^{45,46} The monomer was obtained as slightly brown transparent fluid oil. T_g = -80.5°C (DSC); Anal. Calcd for C₁₅H₂₈F₂N₂O₈S₂ (466.52): C, 38.62%; H, 6.05%; N, 6.00; Found: C, 38.70%; H, 6.12%; N, 5.92%; ¹H NMR (300.13 MHz, CDCl₃): δ = 5.97 (1H, s, CH₂=C Z), 5.48 (1H, m, CH₂=C E), 4.15-4.13 (2H, m, COOCH₂), 3.79 (2H, br. m, OCH₂CH₂N), 3.62-3.59 (2H, m, COOCH₂CH₂), 3.53 (4H, m, OCH₂CH₂O), 3.47-3.42 (6H, m, OCH₂CH₂N, CH₂-2,5), 2.98 (3H, s, N-CH₃), 2.12 (4H, br. m, CH₂-3,4), 1.80 (3H, s, CH₃-C=); ¹³C NMR (100.61 MHz, CDCl₃): δ = 166.9 (C=O), 135.6 (CH₂=C), 125.5 (CH₂=C), 70.0, 69.7, 68.6 (OCH₂), 65.2 (2C, C-2,5), 64.5, 63.5, 63.0 (OCH₂), 48.4 (N-CH₃), 20.9 (2C, C-3,4), 17.8 (CH₃-C=); ¹⁹F NMR (282.40 MHz, CDCl₃): δ = 51.5; IR (KBr pellet): 2958 (m, ν_{C-H}), 2898 (m, ν_{C-H}), 2014 (w), 1925 (w), 1834 (w), 1775 (w), 1715 (s, ν_{C=O}), 1636 (m, ν_{C=C}), 1480 (m), 1458 (m), 1383 (vs), 1364 (s, ν_{asSO2}), 1320 (m), 1296 (m), 1251 (w), 1220 (m), 1180 (vs, ν_{sSO2}), 1105 (vs), 1045 (w), 996 (w), 934 (m), 902 (w), 877 (w), 829 (s),

60 748 (s), 656 (w), 571 (vs), 486 (w), 453 (w) cm⁻¹.

Polymeric ionic liquid (PIL)

ILM (2.00 g, 4.3 mmol), DMF (2.00 g) and AIBN (0.02 g, 1.0 wt.%) were gently mixed in a flask at ambient temperature. The solution was transferred into a glass ampoule. After triple freeze-thaw-pump cycles the ampoule was sealed under vacuum and heated to 60°C for 6 h. The resulting transparent highly viscous polymer solution was slightly diluted with DMF and precipitated into dichloromethane. Polymer was then thoroughly washed with dichloromethane and dried at 70°C/1 mm Hg for 48 h. Yield: 1.31 g (65%); [η]_{0.5M K(FSO₂)₂N in DMF} = 0.55 dL g⁻¹ (25.0 °C); σ_{DC} = 3.4 × 10⁻⁶ S cm⁻¹ (25 °C); T_g = -0.3°C; T_d = 255 °C; IR (thin film on KBr): 2956 (m, ν_{C-H}), 2917 (m, ν_{C-H}), 1724 (s, ν_{C=O}), 1475 (m), 1463 (m), 1382 (vs, ν_{asSO2}), 1360 (vs), 1303 (w), 1270 (m), 1217 (s), 1180 (vs, ν_{sSO2}), 1106 (s), 1037 (w), 998 (w), 935 (w), 829 (s), 747 (s), 572 (vs), 483 (w), 454 (w) cm⁻¹.

Typical semi-IPNs synthesis

NBR (0.135 g) was dissolved in 2.0 mL of 1,1,2- trichloroethane upon stirring at r.t. for 12 h. To the stirred polymer solution the PEGDM (0.080 g), PEGM (0.040 g), ILM (0.240 g) and DCPD (0.0108 g, 3 wt % of methacrylate monomers) were added under inert atmosphere. The resulting solution was then loaded into a mould made from two glass plates clamped together and sealed with a U-shaped Teflon[®] gasket (50.0 mm × 15.0 mm × 0.2 mm). The mould was placed into the thermostat and kept for 5 h at 50 °C, 1 h at 60°C and finally 1 h at 70°C. The resulting film was taken out from the mold and dried for 48 h at 80°C/1 mm Hg.

For semi-IPN2a - semi-IPN2c preparation the respective quantities of [N-Me-N-PrPyr](FSO₂)₂N and lithium bis(trifluoromethylsulfonyl)imide were added to the NBR solution at the same time as methacrylate monomers.

Test cells (full batteries) assembly

Both CR2016 coin-type and coffee-bag-type cells were fabricated. *Anode*: lithium foil (battery grade, with a thickness of 1 mm) was used as a negative electrode. *Cathode*: was fabricated by film casting from the suspension directly on the aluminum (coffee-bag cells) or steel (coin cells) electrodes. The respective mixture was obtained by dissolution of PIL (0.100 g, 22 wt.%), [N-Me-N-PrPyr](FSO₂)₂N (0.100 g, 22 wt.%) and Li(CF₃SO₂)₂N (0.028 g, 6 wt.%) in 1 ml of DMF overnight. To the obtained clear solution the LiFePO₄ (0.205 g, 45 wt.%) and carbon black (0.023 g, 5 wt.%) were added and the resulting slurry was vigorously mixed at r.t. for additional 12 h, whereupon it was poured on the respective electrode surface and the solvent was slowly evaporated at 50 ÷ 60°C. Thin (55-60 μm) polymer cathodes together with metal electrodes were dried at 80°C/1 mmHg for 24 h and further on were used without pressing.

The CR2016 coin-type and coffee-bag cells were fabricated by sandwiching a LiFePO₄ cathode, a polymer electrolyte membrane (semi-IPN2c) and a lithium metal anode in an argon-filled glove box. Electrochemically active surface area was from 0.5 to 3.0 cm², loading of active material varied from 4.2 to 10.5 mg cm⁻² that corresponds to 0.78 - 1.82 mA h cm⁻².

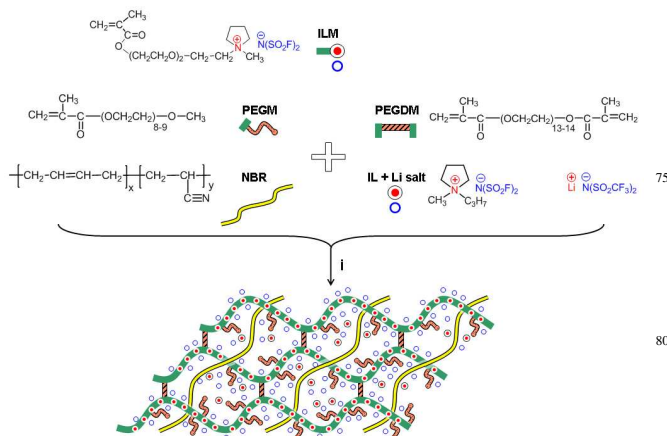
Results and Discussions

Synthesis of ionic liquid like monomer (ILM)

The introduction of new cations and anions coming from ionic liquids chemistry results in virtually unlimited number of possible ILMs variations, hence allowing the control of PILs properties.^{27,28,30} The structure of ILM (Scheme 1) for this study was designed on the basis of our experience in PILs synthesis, investigation of their structure-properties relationships^{21,35–39,47,48} and consideration of literature data^{27–30,32,49} with the main purpose to synthesize highly ionic conducting and electrochemically stable polymers. Thus, the choice of (FSO₂)₂N anion was driven by high ionic conductivity (10⁻³ S cm⁻¹ at 25°C^{50–52}) and outstanding electrochemical stability of ILs based on this anion.^{52,53} The pyrrolidinium cation was selected because among various sets of ILs the combination of cyclic aliphatic cations and imide anions has been found to form the most electrochemically stable electrolyte.⁵⁴ Finally, with consideration for the fact that an increase in the distance between the polymer main chain and the ionic center is favorable for the decrease in PIL's T_g and increase in its ionic conductivity,³⁰ the well-defined flexible oligooxyethylene spacer was chosen (Scheme 1). The synthetic pathway for the preparation of ILM was realized in a similar manner as published by us previously.^{45,48} The structure and purity grade of N-[2-(2-(2-(methacryloyloxy)ethoxy)ethoxy)ethyl]-N-methylpyrrolidinium bis(fluorosulfonyl)imide were proven by ¹H, ¹³C, ¹⁹F NMR, IR spectroscopy and elemental analysis. The synthesized ILM is a viscous brown liquid at r.t. and according to DSC turns to the glassy state at -80.5°C without crystallization. The study of ILM's conductivity revealed a σ_{DC} of 5.5 × 10⁻⁴ S cm⁻¹ (25°C).

Synthesis of ionic semi-interpenetrating networks (semi-IPNs)

The ability of the ILM for radical polymerization was investigated. In a similar manner to its imidazolium analogs^{38,45,46} ILM's bulk polymerization led to the formation of partially cross-linked insoluble polymers. Meanwhile its solution polymerization in DMF afforded for the corresponding linear high molecular PIL. PIL's intrinsic viscosity [η] was found to be 0.55 dL g⁻¹ (0.5 M K(FSO₂)₂N solution in DMF).



Scheme 1 Monomers, polymers, IL and lithium salt used in the preparation of ionic semi-IPNs.

The exchange of FSI anion back to the chloride one allowed the estimation of polymer $M_w = 4.2 \times 10^5 \text{ g mol}^{-1}$ and M_w/M_n to be 4.7. The study of PIL's thermal properties and conductivity gave a $T_g = 0.3^\circ\text{C}$ (TMA), onset mass loss temperature $T_d = 255^\circ\text{C}$ (TGA) and $\sigma_{DC} = 3.4 \times 10^{-6} \text{ S cm}^{-1}$ (25°C). The obtained polyelectrolyte at r.t. represents a rubbery-like material that was not able to keep its shape under the light load.

To improve mechanical properties of PIL and simultaneously to obtain conductive films a new approach consisting in the synthesis of ionic semi-interpenetrating networks was elaborated. In such system ionically conducting network is prepared by copolymerization of ILM with poly(ethylene glycol)(di)methacrylates in the presence of dissolved NBR (Scheme 1). NBR was chosen because of its ability to highly reversible elastic deformations²⁵ and due to the presence of polar nitrile groups,^{55,56} which should ensure the compatibility with ionic network.

NBR solubility probing has shown the 1,1,2-trichloroethane represents a common solvent for all components of semi-IPN, namely ILM, PEGDM, PEGM and NBR. Therefore, this solvent was chosen for the preparation of ionic semi-IPNs with the variable NBR content (Table 1, entries 1-3). Meanwhile ILM : PEGDM : PEGM wt. ratio was fixed at 6 : 2 : 1 as it provides the formation of ionic network without loss of conductivity in comparison with linear PIL.³⁸ It was found that the transformation of viscous monomers/NBR solution into a uniform film occurs under influence of dicyclohexylperoxydicarbonate (DCPD) at 50°C for 7 h with subsequent slow post curing at 60 and 70°C. By such procedure transparent, elastic and self-standing films were fabricated (Fig. 1).



Fig. 1 Appearance of the films based on semi-IPN architecture: photograph of the transparent semi-IPN2 with and without the load.

The typical viscoelastic behavior of ionic semi-IPNs was studied by dynamic mechanical analysis (DMA) and the results are presented in Table 1. As can be seen from Figure 2 the plots of mechanical loss tangent ($\tan \delta$) versus temperature obtained for all semi-IPNs show only a single maximum, thereby indicating the homogeneity of the films at the DMA scale. It was found that the increase of NBR content is accomplished by a small rise of the α relaxation temperature (T_g or T_α) from -1.5 to 3.5°C.

Transmission electron microscopy (TEM) observations were made on **semi-IPN2** samples stained with OsO_4 (Fig. 3, a-b). Since only the butadiene segments of NBR can be marked with OsO_4 , the black regions can be interpreted as NBR-rich phase, while ionic network phase appears as gray regions. In accordance with the TEM pictures, in such film both the elastomer and ionic network partners seem to form continuous phase and are finely distributed in each other, thus proving the semi-IPN architecture. Although a few of white areas of ca. 200 - 300 nm in width can be observed, representing the ionic network phases, the majority of ionic network regions are mainly less than 50 - 60 nm (see Fig. 3, b), which indicates high homogeneity of the film and is consistent with the transparency of the sample.

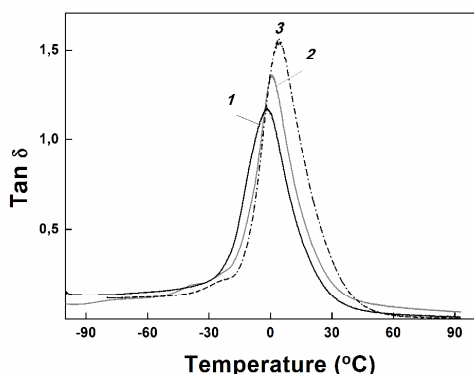


Fig. 2 DMTA analysis for **semi-IPN1** film (1), **semi-IPN2** (2) and **semi-IPN3** (3).

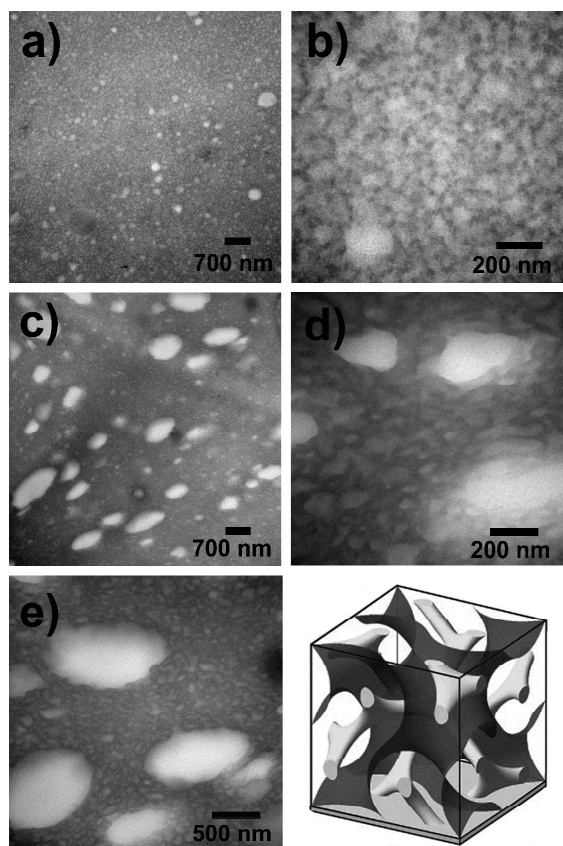


Fig. 3 TEM images of **semi-IPN2** (a, b) and **semi-IPN2c** (c, d, e). Black domains correspond to NBR-rich phase, gray and light-gray domains are

20 attributed to ionic ternary copolymer or ionic network filled with Li salt and IL.

Tensile strength runs show that in contrast to linear PIL, ionic semi-IPNs exhibit perfect mechanical properties (Table 1) that significantly exceed those of linear PIL and cured ILM/PEGDM/PEGM copolymer. Films elongation is 60-180 % and significantly higher than that of ionic network (< 10 %). The same relates to tensile strength, which varied between 180 and 430 kPa for semi-IPNs and was found to be only 115 kPa for respective ionic single network. It was revealed, that both the elongation and tensile strength increased with the growth of NBR fraction (Table 1).

Thermal stability of prepared semi-IPNs was studied by TGA. The onset loss temperature for all films was found to be ~230°C (Table 1 and Fig. 4) that is 65°C higher than for ionic single network³⁸ and slightly less than the T_d of the linear PIL (see vide supra).

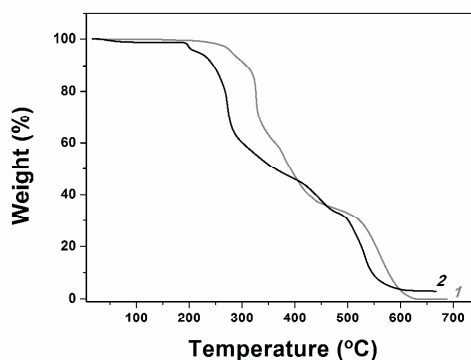


Fig. 4 TGA curves of **semi-IPN2** (1) and **semi-IPN2c** (2) in air (5°C min^{-1}).

The investigation of electrochemical stability was performed by cyclic voltammetry (Fig. 5, curve 1) of **semi-IPN2**. Anodic and cathodic electrochemical evolutions were recorded separately. It was found, that **semi-IPN2** exhibited an electrochemical stability window from c.a. 1.0 to 4.4 V vs Li^+/Li^0 (Table 1). A very low current flow (< $2 \mu\text{A cm}^{-2}$) was observed between the break-down voltages, in support of the high purity of polyelectrolyte.

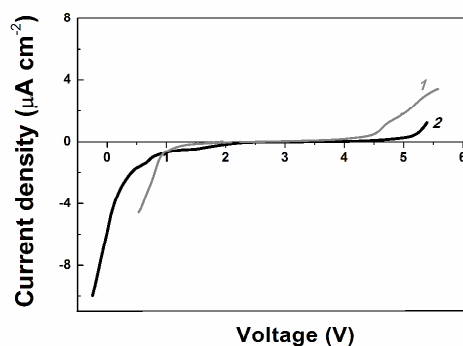


Fig. 5. Electrochemical stability window of **semi-IPN2** (1) and **semi-IPN2c** (2) at 25°C in argon atmosphere (Pt or nickel as working, stainless steel grid as counter electrodes and Li foil as a reference electrodes; scan rate 1 mV s^{-1}).

Finally, the ionic conductivity of semi-IPNs was studied via impedance spectroscopy in anhydrous conditions. It was found that depending on the quantity of NBR fraction the conductivity of semi-IPNs varies in the range from 1.1×10^{-7} to 1.2×10^{-6} S cm^{-1} (25°C). It was found, that the conductivity and mechanical properties show an inverse dependence (Table 1). The higher was the NBR content in the semi-IPN the better were its tensile strength and elongation at break, but the lower was the conductivity.

At this stage of our study, it is possible to conclude that the presence of the linear NBR considerably strengthens mechanical properties of the semi-IPN based films along with the preservation of their thermal characteristics (T_g and T_d) as compared with linear PILs. Films with semi-IPN architecture are soft, flexible, and mechanically resistant. However, the transition from linear PIL to ionic semi-IPNs is accompanied by the decrease of ionic conductivity, most likely due to the overall reduction of the ionic concentration.

Synthesis of filled ionic semi-IPNs

Despite satisfactory mechanical properties semi-IPNs did not meet the requirements for battery applications because they do not contain Li^+ cation needed in electrode reactions and possess insufficient conductivity. Therefore, the filling of semi-IPNs with a lithium salt solution in IL was studied. For better distribution and control of the IL/Li salt uptake the later were added during the polymer synthesis step. N-propyl-N-methylpyrrolidinium bis(fluorosulfonyl)imide IL was chosen to have a common anion with polymer network and because of its high electrochemical stability.^{52,53} The improvement was conducted on **semi-IPN2** as having an optimal balance between the mechanical properties and intrinsic ionic conductivity. For **semi-IPN2a** - **semi-IPN2c** synthesis the concentration of IL was varied from 15 to c.a. 44 wt. % (Table 2), while the concentration of the Li salt was invariable and equal to 12.4 wt. %. The obtained filled semi-IPNs (**semi-IPN2a** - **semi-IPN2c**) represented transparent, elastic and tough films. No phase separation phenomenon, i.e., ionic liquid release, was observed for the samples within prolonged storage (3 months), thus suggesting a high physico-chemical stability of prepared films.

The study of filled semi-IPNs by DMA demonstrates a single maximum on the temperature dependence of $\tan \delta$ (Fig. 6), standing for good homogeneity of the films at the DMA scale.

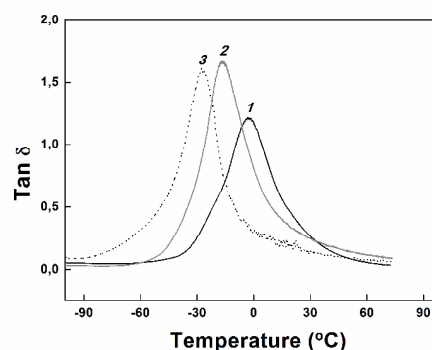


Fig. 6 DMTA analysis for **semi-IPN2a** (1), **semi-IPN2b** (2) and **semi-IPN2c** (3).

The introduction of IL/Li salt mixture into the polymer matrix reduces its thermal properties in comparison with **semi-IPN2** (Tables 1 and 2). The increase of IL content from 15 to 43.8 wt. % leads to the significant reduction of polymer material's T_g to -27.3°C (Table 2, entries 1-3) and slight decrease of its onset mass loss temperature (Fig. 4, curve 2). The introduction of IL/Li salt mixture affects mechanical properties of the synthesized films as well, decreasing their tensile strength and elongation (Table 1, entry 2 and Table 2, entries 1-3). However, at the same time, the presence of IL and Li salt as additional source of ions significantly increases ionic conductivity of the film reaching 10^{-4} S cm^{-1} level for **semi-IPN2c** at 25°C. Further study of temperature versus ionic conductivity dependence for **semi-IPN2c** revealed its non linear (free-volume) character (Fig. 7). The conductivity of **semi-IPN2c** increases with temperature which can be explained by an increase in the mobility of charge carriers and the mobility of the polymer chain. Thus, at 40°C the ionic conductivity of film is equal to 5.0×10^{-4} S cm^{-1} double that at 25°C. The increase of conductivity by one order of magnitude (10^{-3} S cm^{-1}) is already observed at 80°C.

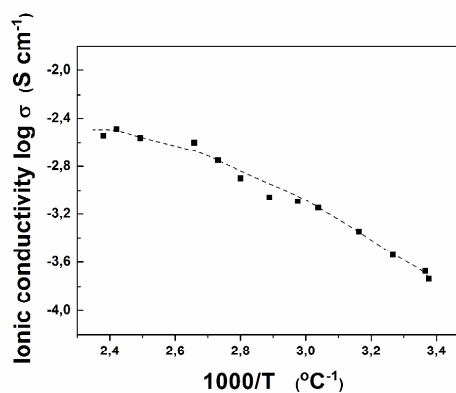


Fig. 7 Temperature dependence of ionic conductivity for **semi-IPN2c** film.

The electrochemical stability window for the **semi-IPN2c** was measured by cyclic voltamperometry (Fig. 5, curve 2). It reveals that the electrochemical stability of the **semi-IPN2c** is higher than that of its unfilled analogue (**semi-IPN2**). The found electrochemical window versus Li/Li^+ was found to be 4.9 V. This result clearly demonstrates that **semi-IPN2c** based polymer electrolyte has excellent electrochemical stability, thus confirming its feasibility for application in various electronics,

including lithium batteries.

The morphology of the **semi-IPN2c** film, synthesized in the presence of IL and lithium salt was examined by TEM (Fig. 3, c-e). Similarly to **semi-IPN2**, the continuous phase in **semi-IPN2c** is formed by NBR and a very finely distributed small (0 - 20 nm) ionic network domains are still present and uniformly intertwine with elastomer. At the same time large ionic domains with a diameter from 200 to 700 nm, representing a gel made of ILM/PEGDM/PEGM copolymer filled with IL/Li salt mixture, are clearly observed leading to the conclusion that the presence of IL and lithium salt during the film's synthesis promotes some phase separation and the formation of "Emmentaler cheese" like structure. Nevertheless, since rather high conductivity and ions mobility have been found for **semi-IPN2c**, it can be assumed the major part of ionic network is involved in interconnection and forms second continuous phase.

To demonstrate the superiority of the semi-IPNs they were compared with close polymer analogues representing linear PILs filled with ILs and Li salts (Table 2, entries 3 and 4-5). For example, as it can be seen from Table 2, the ionic conductivity of **semi-IPN2c** reaches 10^{-4} S cm⁻¹ at a lower level of Li salt/IL solution addition than linear PILs. The electrochemical stability coincides with similar analogues (Table 2, entries 3 and 4). At the same time, filled semi-IPNs demonstrate perfect mechanical properties, in particular superior elongation at break, i.e. superior elasticity (Table 2, entry 3). Thus, it can be concluded that the suggested technology, consisting in the semi-IPN architecture, unreservedly proved its effectiveness in terms of simultaneous imparting of high conductivity and good mechanical properties to the single polymer film.

Application as solid electrolyte in Li/LiFePO₄ batteries

To show one of the possible practical applications, the prepared **semi-IPN2c** films were tested as solid flexible electrolytes in Li/LiFePO₄ batteries.

The study started from the investigation of films chemical stability. The later and the interfacial properties of **semi-IPN2c** at the interface with the metal lithium were evaluated by following the time evolution of the impedance response of symmetrical Li/**semi-IPN2c**/Li cells stored at 25 and 40°C (Fig. 8). Figure 8 (a and c) shows the high frequency region of AC responses for the Li/**semi-IPN2c**/Li cells as made and subsequently after 4, 11, 20, 33, 100, 106 and 115 days of storage at these respective temperatures. The intercept of the curves with the real axis corresponds to the polymer electrolyte bulk ionic resistance.⁵⁷ As it can be seen from Fig. 8a, during the initial period of storage at 25°C an increase of the resistance was observed. However, the impedance response became stable after 100 days of storage. In contrast, at 40°C the AC measure of the Li/**semi-IPN2c**/Li cells was already stable after 20 days (Fig. 8, c). This can be attributed to the initial reaction between the lithium electrode and the **semi-IPN2c** electrolyte to form a passive layer (Solid Electrolyte Interphase, SEI)⁵⁷ on the surface of the lithium anode that protects the electrode from further reaction. At 25°C the formation of SEI takes longer time than at elevated temperature.

However, the stability of AC response beyond a given time of storage indicates that no degradation phenomenon takes place with **semi-IPN2c** polymer electrolyte in contact with metallic lithium.

Figures 8b and 8d display the Nyquist plot of Li/**semi-IPN2c**/Li cells kept at 25 and 40°C for prolonged time. All **semi-IPN2c** based polymer electrolytes showed depressed semicircles that are associated with Li-polymer interfacial processes. The diameters of the semicircles are often attributed to the overall interfacial resistance that includes the charge transfer resistance at the Li/polymer electrolyte interface and the resistance associated with the growth of a passive layer.⁵⁷⁻⁵⁹ Again, at the initial period of storage at 25°C an increase of interfacial resistance was observed until the AC plot became constant after ~30 days of storage. This behavior can be attributed directly to the SEI

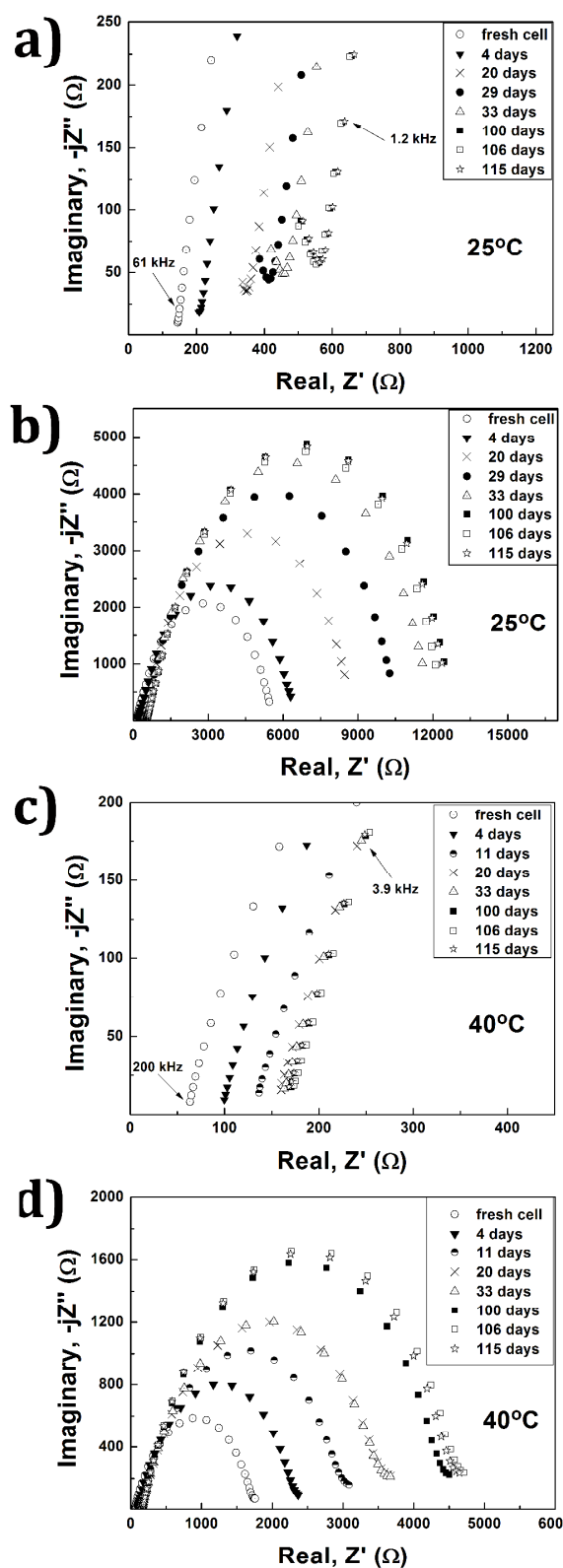


Fig. 8 AC responses of a symmetrical Li/semi-IPN2c/Li cell stored under different temperature conditions: 25°C (*a, b*) and 40°C (*c, d*).

formation as frequently reported for the solvent-free polymer electrolytes.^{57,59,60} Figures 8b and 8d clearly show that the increase in the cells temperature from 25 to 40°C leads to the

pronounced reduction of semicircles diameter and, in its turn, to the decrease of polymer interfacial resistance.

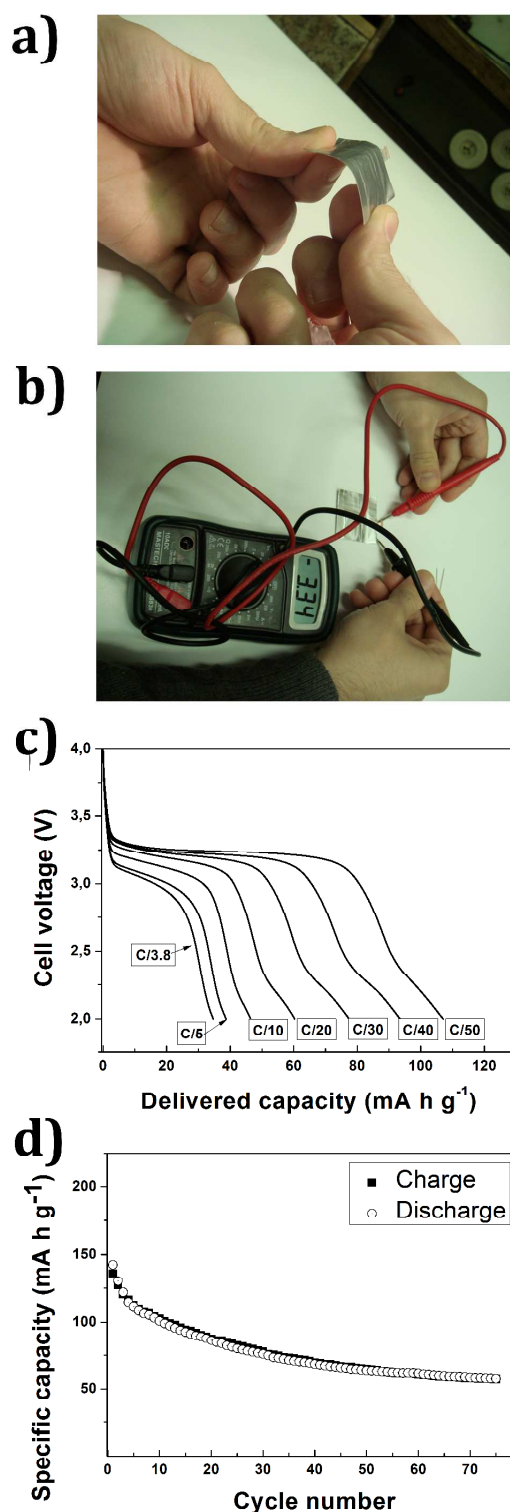


Fig. 9 Appearance and characterization at 40°C of the thin film Li/semi-IPN2c/LiFePO₄ coffee-bag batteries: photograph of the thin flexible battery (*a* and *b*); voltage vs. delivered capacity profile of selected discharge half-cycles with variable discharge rate from C/50 to C/3.8 at a constant charge rate of C/50 (7.8 μA h) (*c*) and cycling performance of the battery with a charge rate C/50 (7.8 μA h) (*d*).

Further on the full Li/LiFePO₄ batteries with semi-IPN2c films as polymer separator were assembled (Fig. 9, a and b), and their cycling performance was characterized at 40°C (Fig. 9, b and c). Figure 9b depicts the voltage versus capacity dependence of the discharge half-cycles obtained at various current rates. The discharge process occurs at 3.20 - 3.25 V, showing the flat plateau up to C/20 discharge rates. At higher discharge rates (C/10 - C/3.8) the flat voltage region is progressively shortening and shifting down to 3.0 V (Fig. 9, b). In another test, the cell underwent 75 charge/discharge cycles at a constant C/50 charge/discharge rate (Fig. 9, c). The maximum delivered capacity was equal to 142 mA h g⁻¹ during the first discharged cycle. Then a gradual decrease of the capacity was observed till it became nearly constant (from 69 to 60 mA h g⁻¹) after 40th discharge cycle. An average specific capacity of the semi-IPN2c based Li/LiFePO₄ battery for 75 charge/discharge cycles at 40°C was found to be 77 mA h g⁻¹.

Conclusions

The formation of a series of polymer films, representing semi-interpenetrating polymer networks (semi-IPNs) with chemically attached ionic groups was studied. Such ionic semi-IPNs were developed using simple one-step process. At this, the ionic network, formed by radical copolymerization of ionic liquid like monomer (N-[2-(2-(2-(methacryloyloxy)ethoxy)ethoxy)ethyl]-N-methylpyrrolidinium bis(fluorosulfonyl)imide) with poly(ethylene glycol)(di)methacrylates, acts as a solid polymer electrolyte, whereas nitrile butadiene rubber (NBR) ensures the reinforcement of mechanical properties.

In the unfilled state the semi-IPN with the 20 wt.% of NBR content shows the best compromise between perfect mechanical properties (tensile strength: 290 kPa, elongation: 150 %) and ionic conductivity of 8.0×10^{-7} S cm⁻¹ at 25°C. Semi-IPNs of the same composition filled with 44 wt.% of N-propyl-N-methylpyrrolidinium bis(fluorosulfonyl)imide and 12 wt.% of lithium bis(trifluoromethylsulfonyl)imide demonstrate an ionic conductivity higher than 10^{-4} S cm⁻¹ (25°C), while maintaining a tensile strength of 80 kPa and an elongation of 60 %.

The most striking advantages of the suggested approach in comparison with linear polymeric ionic liquids are: (1) significant improvement in the stress-strain properties of the films even in the filled state; (2) lowering of polymer T_g and increasing of the ions mobility; (3) imparting of high ionic conductivity (up to 1.3×10^{-4} S cm⁻¹ at 25°C) and (4) preservation of high electrochemical stability window (4.9 V versus Li/Li⁺).

Preliminary battery tests have demonstrated that Li/LiFePO₄ flexible cells with semi-IPN based electrolyte are capable to deliver a 77 mA h g⁻¹ average specific capacity at 40°C during 75 charge/discharge cycles, thus making the films with semi-IPN architecture promising candidates for stretchable electronics.

Acknowledgements

This work was supported by the Russian Foundation for Basic Research (projects no. 13-03-00343-a, 14-03-31953_mol_a and

14-29-0403914_ofi_m) and by European Commission through the International Research Staff Exchange Scheme (FP7-PEOPLE-2012-IRSES, project no. 318873 «IONRUN»). Alexander S. Shaplov is grateful to the University of Cergy-Pontoise for the sponsorship of his visit and work in the LPPI laboratory. Authors would like to thank Dr. Isabelle Anselme-Bertrand (Centre de Microscopie Electronique Stéphanois (CMES)) for TEM measurements, Prof. C. Wandrey (Laboratoire de Médecine Régénérative et de Pharmacobiologie, Ecole Polytechnique Fédérale de Lausanne) for the providing of poly(diallyldimethylammonium) chloride, Advanced Lithium Electrochemistry Co., Ltd. for a generous gift of LiFePO₄ and Prof. A.A. Askadskii along with V.V. Kazantseva (A.N. Nesmeyanov Institute of Organoelement Compounds, Russian Academy of Sciences) for mechanical characterization of prepared films.

Notes and references

- ^a A.N. Nesmeyanov Institute of Organoelement Compounds Russian Academy of Sciences (INEOS RAS), Vavilov str. 28, 119991, GSP-1, Moscow, Russia. Fax: +7 499 1355085; Tel: +7 499 1359244; E-mail: shaplov@ineos.ac.ru (A.S. Shaplov)
- ^b Department of Macromolecular Chemistry, Saint-Petersburg State University, Universitetsky pr. 26, 198504, Saint-Petersburg, Russia
- ^c Laboratoire de Réactivité et Chimie des Solides (LRCS), University of Picardie Jules Verne, UMR 6007 CNRS, 33 rue de Saint-Leu, 80039 Amiens, France
- ^d Laboratoire de Physico-chimie des Polymères et des Interfaces (LPPI), Université de Cergy-Pontoise, 5 mail Gay-Lussac, 95031 Cergy-Pontoise Cedex, France
- 1 S. R. Forrest and M. E. Thompson, *Chem. Rev.*, 2007, **107**, 923–925.
- 2 A. R. Murphy and J. M. J. Fréchet, *Chem. Rev.*, 2007, **107**, 1066–1096.
- 3 H. Zhou, L. Yang and W. You, *Macromolecules*, 2012, **45**, 607–632.
- 4 N. S. Ilicheva, N. K. Kitaeva, V. R. Dufлот and V. I. Kabanova, *ISRN Polym. Sci.*, 2012, **2012**, 1–7.
- 5 F. Xu and Y. Zhu, *Adv. Mater.*, 2012, **24**, 5117–5122.
- 6 H.-W. Liang, Q.-F. Guan, Z.-Zhu, L.-T. Song, H.-B. Yao, X. Lei and S.-H. Yu, *NPG Asia Mater.*, 2012, **4**, e19.
- 7 Q. Yuan, S. A. Bateman, S. Shen, C. Gloria-Esparza and K. Xia, *J. Thermoplast. Compos. Mater.*, 2013, **26**, 30–43.
- 8 Y. Li, L. Zhao and H. Shimizu, *Macromol. Rapid Commun.*, 2011, **32**, 289–294.
- 9 A. Saleem, L. Frommann and A. Soever, *Polymers*, 2010, **2**, 200–210.
- 10 J.-C. Huang, *Adv. Polym. Technol.*, 2002, **21**, 299–313.
- 11 D. T. Hallinan and N. P. Balsara, *Annu. Rev. Mater. Res.*, 2013, **43**, 503–525.
- 12 R. C. Agrawal and G. P. Pandey, *J. Phys. Appl. Phys.*, 2008, **41**, 223001.
- 13 M. P. Singh, R. K. Singh and S. Chandra, *Prog. Mater. Sci.*, 2014, **64**, 73–120.
- 14 F. M. Gray, Ed., *Solid polymer electrolytes: fundamentals and technological applications.*, Wiley-VCH, New York, 1991.
- 15 M. A. Ratner and D. F. Shriver, *Chem Rev*, 1988, **88**, 109–124.
- 16 G. Beaucage, S. Rane, D. W. Schaefer, G. Long and D. Fischer, *J. Polym. Sci. Part B Polym. Phys.*, 1999, **37**, 1105–1119.
- 17 G. Wu and Q. Zheng, *J. Polym. Sci. Part B Polym. Phys.*, 2004, **42**, 1199–1205.
- 18 N. Winterton, *J Mater Chem*, 2006, **16**, 4281–4293.
- 19 M. Forsyth, S. Jiazeng and D. . MacFarlane, *Electrochimica Acta*, 2000, **45**, 1249–1254.
- 20 A. Noda and M. Watanabe, *Electrochimica Acta*, 2000, **45**, 1265–1270.

- 21 A. S. Shaplov, L. Goujon, F. Vidal, E. I. Lozinskaya, F. Meyer, I. A. Malyshkina, C. Chevrot, D. Teyssié, I. L. Odinet and Y. S. Vygodskii, *J. Polym. Sci. Part Polym. Chem.*, 2009, **47**, 4245–4266.
- 22 S. Savagatrup, A. D. Printz, T. F. O'Connor, A. V. Zaretski and D. J. Lipomi, *Chem. Mater.*, 2014, **26**, 3028–3041.
- 23 F. Vidal, C. Plesse, D. Teyssié and C. Chevrot, *Synth. Met.*, 2004, **142**, 287–291.
- 24 F. Vidal, C. Plesse, G. Palaprat, A. Kheddar, J. Citerin, D. Teyssié and C. Chevrot, *Synth. Met.*, 2006, **156**, 1299–1304.
- 25 L. J. Goujon, A. Khaldi, A. Maziz, C. Plesse, G. T. M. Nguyen, P.-H. Aubert, F. Vidal, C. Chevrot and D. Teyssié, *Macromolecules*, 2011, **44**, 9683–9691.
- 26 H. Ohno and M. Yoshizawa, in *Ionic Liquids IIIB: Fundamentals, Progress, Challenges, and Opportunities: Transformations and Processes*, American Chemical Society, Washington, DC, 2005, pp. 159–170.
- 27 H. Ohno, *Macromol. Symp.*, 2007, **249–250**, 551–556.
- 28 M. D. Green and T. E. Long, *Polym. Rev.*, 2009, **49**, 291–314.
- 29 O. Green, S. Grubjesic, S. Lee and M. A. Firestone, *Polym. Rev.*, 2009, **49**, 339–360.
- 30 A. S. Shaplov, E. I. Lozinskaya and Y. S. Vygodskii, in *Chapter 9 'Polymer Ionic Liquids: Synthesis, Design and Application in Electrochemistry as Ion Conducting Materials' in Electrochemical Properties and Applications of Ionic Liquids*, eds. A. A. J. Torriero and M. J. A. Shiddiky, Novapublishers, New York, 2010, pp. 203–298.
- 31 D. Mecerreyes, *Prog. Polym. Sci.*, 2011, **36**, 1629–1648.
- 32 J. Yuan and M. Antonietti, *Polymer*, 2011, **52**, 1469–1482.
- 33 J. Yuan, D. Mecerreyes and M. Antonietti, *Prog. Polym. Sci.*, 2013, **38**, 1009–1036.
- 34 Y. S. Vygodskii, A. S. Shaplov, E. I. Lozinskaya, P. S. Vlasov, I. A. Malyshkina, N. D. Gavrilova, P. Santhosh Kumar and M. R. Buchmeiser, *Macromolecules*, 2008, **41**, 1919–1928.
- 35 A. S. Shaplov, E. I. Lozinskaya, D. O. Ponkratov, I. A. Malyshkina, F. Vidal, P.-H. Aubert, O. V. Okatova, G. M. Pavlov, L. I. Komarova, C. Wandrey and Y. S. Vygodskii, *Electrochimica Acta*, 2011, **57**, 74–90.
- 36 A. S. Shaplov, P. S. Vlasov, E. I. Lozinskaya, D. O. Ponkratov, I. A. Malyshkina, F. Vidal, O. V. Okatova, G. M. Pavlov, C. Wandrey, A. Bhide, M. Schönhoff and Y. S. Vygodskii, *Macromolecules*, 2011, **44**, 9792–9803.
- 37 A. S. Shaplov, P. S. Vlasov, M. Armand, E. I. Lozinskaya, D. O. Ponkratov, I. A. Malyshkina, F. Vidal, O. V. Okatova, G. M. Pavlov, C. Wandrey, I. A. Godovikov and Y. S. Vygodskii, *Polym Chem*, 2011, **2**, 2609–2618.
- 38 A. S. Shaplov, D. O. Ponkratov, P. S. Vlasov, E. I. Lozinskaya, L. I. Komarova, I. A. Malyshkina, F. Vidal, G. T. M. Nguyen, M. Armand, C. Wandrey and Y. S. Vygodskii, *Polym. Sci. Ser. B*, 2013, **55**, 122–138.
- 39 Y. S. Vygodskii, A. S. Shaplov, E. I. Lozinskaya, K. A. Lyssenko, D. G. Golovanov, I. A. Malyshkina, N. D. Gavrilova and M. R. Buchmeiser, *Macromol. Chem. Phys.*, 2008, **209**, 40–51.
- 40 Rus. Pat., 2503098, 2013.
- 41 WO Pat., 2014/006333, 2014.
- 42 F. Vidal, J. Jüger, C. Chevrot and D. Teyssié, *Polym. Bull.*, 2006, **57**, 473–480.
- 43 N. Bar, K. Ramanjaneyulu and P. Basak, *J. Phys. Chem. C*, 2014, **118**, 159–174.
- 44 J.-M. Kim, J.-H. Park, C. K. Lee and S.-Y. Lee, *Sci. Rep.*, 2014, **4**.
- 45 A. S. Shaplov, D. O. Ponkratov, P.-H. Aubert, E. I. Lozinskaya, C. Plesse, F. Vidal and Y. S. Vygodskii, *Chem. Commun.*, 2014, **50**, 3191.
- 46 A. S. Shaplov, D. O. Ponkratov, P.-H. Aubert, E. I. Lozinskaya, C. Plesse, A. Maziz, P. S. Vlasov, F. Vidal and Y. S. Vygodskii, *Polymer*, 2014, **55**, 3385–3396.
- 47 A. S. Shaplov, E. I. Lozinskaya, R. Losada, C. Wandrey, A. T. Zdvizhkov, A. A. Korlyukov, K. A. Lyssenko, I. A. Malyshkina and Y. S. Vygodskii, *Polym. Adv. Technol.*, 2011, **22**, 448–457.
- 48 A. S. Shaplov, D. O. Ponkratov, P. S. Vlasov, E. I. Lozinskaya, I. A. Malyshkina, F. Vidal, P.-H. Aubert, M. Armand and Y. S. Vygodskii, *Vysokomol. Soed. (Polym. Sci. J.) Ser. B*, 2014, **56**, 164–177.
- 49 A. Laschewsky, *Curr. Opin. Colloid Interface Sci.*, 2012, **17**, 56–63.
- 50 M. Ishikawa, T. Sugimoto, M. Kikuta, E. Ishiko and M. Kono, *J. Power Sources*, 2006, **162**, 658–662.
- 51 Q. Zhou, W. A. Henderson, G. B. Appetecchi, M. Montanino and S. Passerini, *J Phys Chem B*, 2008, **112**, 13577–13580.
- 52 E. Paillard, Q. Zhou, W. A. Henderson, G. B. Appetecchi, M. Montanino and S. Passerini, *J. Electrochem. Soc.*, 2009, **156**, A891–A895.
- 53 H.-B. Han, S.-S. Zhou, D.-J. Zhang, S.-W. Feng, L.-F. Li, K. Liu, W.-F. Feng, J. Nie, H. Li, X.-J. Huang, M. Armand and Z.-B. Zhou, *J. Power Sources*, 2011, **196**, 3623–3632.
- 54 H. Matsumoto, H. Sakaebe and K. Tatsumi, *J. Power Sources*, 2005, **146**, 45–50.
- 55 E. Marwanta, T. Mizumo, N. Nakamura and H. Ohno, *Polymer*, 2005, **46**, 3795–3800.
- 56 E. Marwanta, T. Mizumo and H. Ohno, *Solid State Ion.*, 2007, **178**, 227–232.
- 57 M. E. Orazem and B. Tribollet, *Electrochemical impedance spectroscopy*, Wiley, Hoboken, N.J., 2008.
- 58 G.-T. Kim, G. B. Appetecchi, F. Alessandrini and S. Passerini, *J. Power Sources*, 2007, **171**, 861–869.
- 59 G. B. Appetecchi, G.-T. Kim, M. Montanino, M. Carewska, R. Marcilla, D. Mecerreyes and I. De Meatza, *J. Power Sources*, 2010, **195**, 3668–3675.
- 60 G. B. Appetecchi and S. Passerini, *J. Electrochem. Soc.*, 2002, **149**, A891.
- 61 K. Yin, Z. Zhang, L. Yang and S.-I. Hirano, *J. Power Sources*, 2014, **258**, 150–154.

Cite this: DOI: 10.1039/c0xx00000x

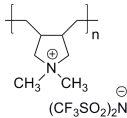
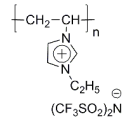
ARTICLE TYPE

www.rsc.org/xxxxxx

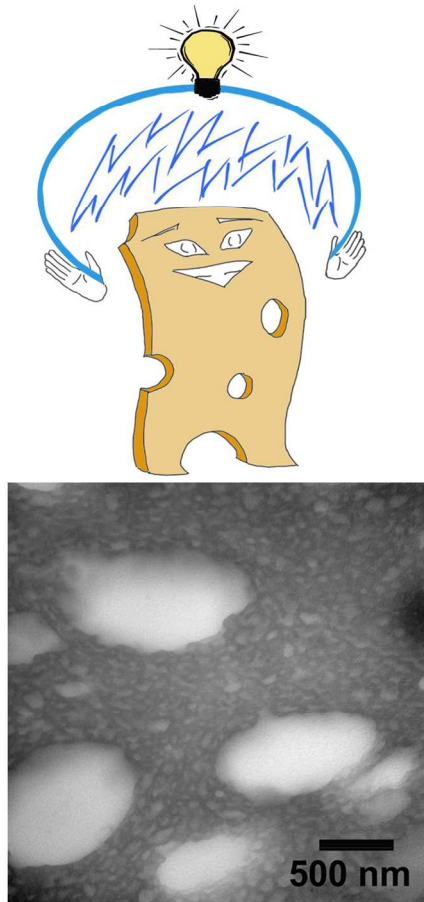
Table 1 Properties of ionic semi-IPNs

no	Name	Composition				Properties						
		ILM (wt.%)	PEGDM (wt.%)	PEGM (wt.%)	NBR (wt.%)	$T_g(T_a)$ (°C) ^a	σ_t (kPa) ^b	E_t (kPa) ^c	ϵ_t (%) ^d	T_d (°C) ^e	EW (V) ^f	σ_{DC} (S cm ⁻¹)
1	semi-IPN1	46.8	15.5	7.7	30.0	3.5	430	550	180	245	-	1.1×10^{-7}
2	semi-IPN1	53.5	17.7	8.8	20.0	0.8	290	420	150	225	3.4	8.0×10^{-7}
3	semi-IPN1	60.0	20.0	10.0	10.0	-1.5	180	1500	60	225	-	1.2×10^{-6}

^a Determined by DMTA. ^b Tensile strength. ^c Tensile modulus. ^d Elongation. ^e Onset loss temperature by TGA. ^f Electrochemical stability window.**Table 2** Properties of filled semi-IPN2.

no	Name	Polymer electrolyte										Ref.	
		Composition				Properties							
		Polymer matrix Type	IL (wt.%)	Li(CF ₃ SO ₂) ₂ N (wt.%)	σ_{DC} (S cm ⁻¹) 20°C/40°C	EW (V) ^a	σ_t (kPa) ^b	E_t (kPa) ^c	ϵ_t (%) ^d	$T_g(T_a)$ (°C) ^e	T_d (°C) ^f		
1	semi-IPN2a	ionic semi-IPN	72.6	15.0	12.4	1.1×10^{-5}	-	280	780	45	-7.6	225	-
2	semi-IPN2b		60.0	27.6	12.4	3.6×10^{-5}	-	150	450	50	-16.8	215	-
3	semi-IPN2c		43.8	43.8	12.4	$1.3 \times 10^{-4}/3.5 \times 10^{-4}$	4.9	80	240	60	-27.3	190	-
4 ^g	polyDADMAB		27.6	60.0	12.4	$1.6 \times 10^{-4}/4.8 \times 10^{-4}$	5.0	60 ^h	1150 ^h	10 ^h	-67; 12 -53.9; 1.6 ^h	350	59
5 ^g	poly-N-vinylim		54.5	35.0	10.5	$1.9 \times 10^{-5}/6.3 \times 10^{-5}$	2.3	Sticky mass			-26.9 ^{hi}	325	61

^a Electrochemical stability window. ^b Tensile strength. ^c Tensile modulus. ^d Elongation. ^e Determined by DMTA. ^f Onset loss temperature by TGA. ^g For comparison. ^h Measured in this work. ⁱ Determined by TMA.



TOC

